Magnetically assisted quantum cascade laser emitting from 740 GHz to 1.4 THz

Giacomo Scalari,[a] Dana Turčinková, James Lloyd-Hughes, Maria I. Amanti, Milan Fischer, Mattias Beck, and Jérôme Faist
Institute of Quantum Electronics, ETH Zurich, Zurich 8093, Switzerland

(Received 28 June 2010; accepted 2 August 2010; published online 25 August 2010)

In this paper we show that by applying a perpendicular magnetic field to a quantum cascade structure it is possible to enhance the gain of different optical transitions. The combination of magnetic confinement with a broadband, cutoff-free optical resonator allows the demonstration of laser action over a large bandwidth, from 733 GHz to 1.38 THz together with the emission at 3.2 THz. A different lasing scheme is revealed that does not rely on resonant tunneling as the main injection mechanism. In combination with the magnetically enhanced gain laser emission at 1 THz is observed up to a temperature of 115 K, which corresponds to a ratio $k_BT/h\nu=2.3$ between the lattice thermal energy and the laser photon energy. © *2010 American Institute of Physics*. [doi:10.1063/1.3481698]

The application of a strong magnetic field perpendicular to the plane of the layers has provided valuable informations about the dominant scattering mechanisms active in quantum cascade laser (QCL) (Ref. 1) structures.[2] In the terahertz (THz) range, where the photon energy $h\nu$ is smaller than the LO phonon energy $\hbar\omega_{LO}$, the device performance are dramatically modified by the change in the density of states induced by the magnetic field. The suppression of the nonradiative relaxation channels has allowed the observation of threshold current densities below 1 A/cm^2 for fields above 12 T[3,4] and an increase in the operating temperature up to 225 K in very strong fields above 19 T and higher.[5]

We show that magneto-spectroscopy can also be used to enhance the gain of different optical transitions in the structure and, combined with a low loss, broadband optical resonator, reveal different lasing schemes. We investigate the role of magnetic confinement on a simple THz QCL structure based on a step-well and described in Ref. 6. The experimental setup used for the investigation is described in Ref. 3. A color plot of the laser emission intensity as a function of the injected current and applied magnetic field starting from 2.7 T is reported in Fig. 1(b). In panel (a) of the same figure a Landau fan is shown for the two levels that constitute the upper and lower lasing states for the 3.2 THz emission. Adopting the same labeling as in Ref. 6, the laser emits at 12.8 meV (3–3.2 THz) when the optical transition is intrawell from levels $|5\rangle \rightarrow |4\rangle$. From the plot of Fig. 1(b) we can observe the modulations of the laser threshold and the laser intensity due to intersubband Landau level resonances[3] when injecting electrons in state $|5\rangle$ (B=4.1 T corresponds to $\hbar\omega_c=2\cdot E_{54}$ where $\omega_c=eB/m^*$). The laser action for the $|5\rangle \rightarrow |4\rangle$ transition is entirely suppressed when $\hbar\omega_c=E_{54}$, for B field values ranging from 7–9.2 T. Laser action at E_{54} starts again at 9.5 T. As a function of the injected current, laser action stops when the injector state $|1'\rangle$ is in full resonance with the upper state $|5\rangle$ and the I-V curve presents the characteristic negative differential resistance (NDR) feature (calculated electric field F=6.7 kV/cm). Before 4 T the laser signal after the NDR is still due to the $|5\rangle \rightarrow |4\rangle$ transition; the measurement is in pulsed mode and the edges of the pulse can switch on and off the laser creating this signal after the NDR. This signal cannot be discriminated because of the slow response of the He-cooled Si-bolometer (45 Hz) which does not allow for a time gating of the optical signal.

At fields between 4.3 and 8.5 T there is a change in the observed optical signal, which results more clearly from the sections at constant magnetic field reported in Fig. 1(c)–1(e). Such a change reflects the onset of laser action on another optical transition emitting at low THz frequencies. Spectral measurements were carried out and the observed laser spans almost an octave in frequency, starting at 3.03 meV (733 GHz) up to 5.72 meV (1.38 THz). The laser emission can be tuned by a combination of magnetic field and applied bias, [see Fig. 2(c)]. In Fig. 2(a) we report a bandstructure calculation for an applied electric field of 8.5 kV/cm, (above the calculated NDR value of 6.7 kV/cm), together with a schematic of the physical process that can create the gain at such low THz frequencies. The $|1'\rangle \rightarrow |5\rangle$ transition is strongly diagonal in real space ($z_{1'1'}$-z_{55}=26.6 nm) and can present a high population inversion because, at low temperatures, after the NDR the electrons tend to cumulate in the upper state $|1'\rangle$, due to the relatively low wave function overlap with the lower state $|5\rangle$. The lower state is depleted by means of intersubband scattering on the transition $|5\rangle \rightarrow |4\rangle$. Being the energy $E_{1'5}$ very low, the resonance condition $\hbar\omega_c=E_{1'5}$ is satisfied already at B=2.5 T and the observed modulation of the laser emission $E_{1'5}$ from the magnetic field is due to lower state lifetime modulation. When the cyclotron energy is resonant with the E_{54} energy (B=7–7.5 T), which constitutes the extraction stage of the $|1'\rangle \rightarrow |5\rangle$ laser, we indeed observe a maximum in the laser intensity.[7] We noted that also the $|4\rangle \rightarrow |3\rangle$ diagonal transition could be responsible of the observed low frequency THz emission, with state $|3\rangle$ depopulated by phonon scattering. In Fig. 2(d) we report the calculated energy shift as a function of the applied electric field for both $|4\rangle \rightarrow |3\rangle$ and $|1'\rangle \rightarrow |5\rangle$. Population inversion of transition $|4\rangle \rightarrow |3\rangle$ is modulated in the same way as $|1'\rangle \rightarrow |5\rangle$ because the Landau resonance $\hbar\omega_c=E_{54}$ increases the upper state $|4\rangle$ population. A calculation of the populations of level $|4\rangle$ is beyond the scope of this paper but we can specu-

[a]Electronic mail: scalari@phys.ethz.ch.

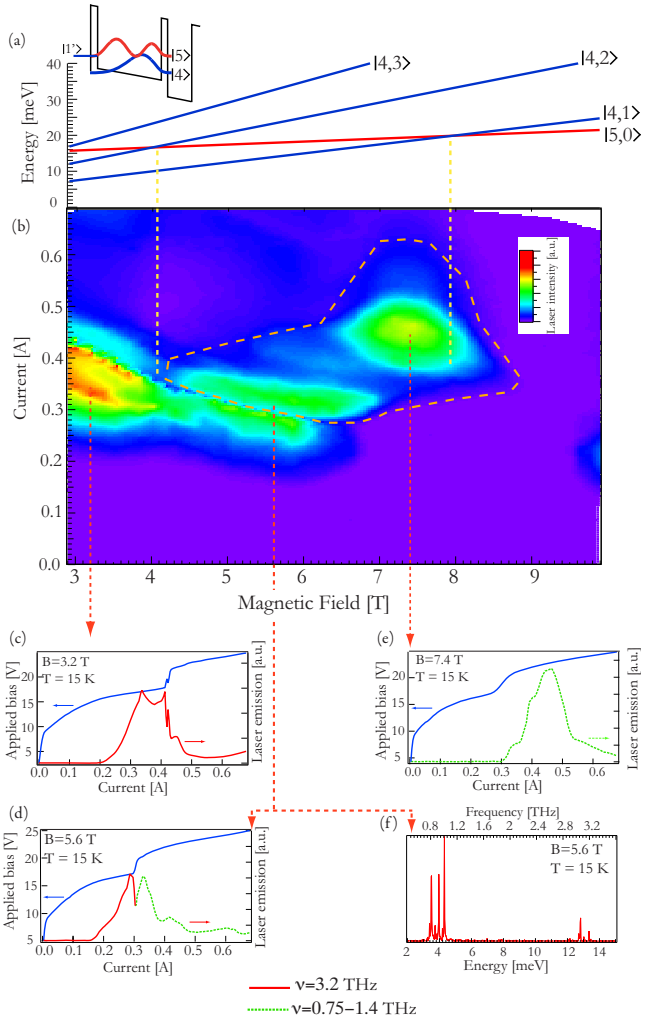

FIG. 1. (Color online) (a) Landau fan plot of the laser levels corresponding to the main transition at 12.5 meV. Inset: scheme of the active well for the 3.2 THz emission. (b) Laser emission as a function of the applied magnetic field (in the region 2.7–10 T) and the injected current for a Fabry–Pérot double-metal cavity (1.6 mm long, 100 μm wide) measured at T=15 K. The region highlighted by an orange dashed line corresponds to the laser emission from levels $|1'\rangle \rightarrow |5\rangle$. The vertical dashed yellow lines highlight the resonances between Landau levels $|5,0\rangle \rightarrow |4,2\rangle$ and $|5,0\rangle \rightarrow |4,1\rangle$. (c) L-I-V curve at 3.2 T and 15 K. (d) L-I-V curve at 5.6 T and 15 K. (e) L-I-V curve at 7.4 T and 15 K. It is evident the progressive turn on of the diagonal laser transition $|1'\rangle \rightarrow |5\rangle$ (dashed line, as indicated in the inset) after the NDR feature. (f) Spectral emission at 5.3 T for an injected current of 0.35 A: the two laser emissions are visible but they are not simultaneous.

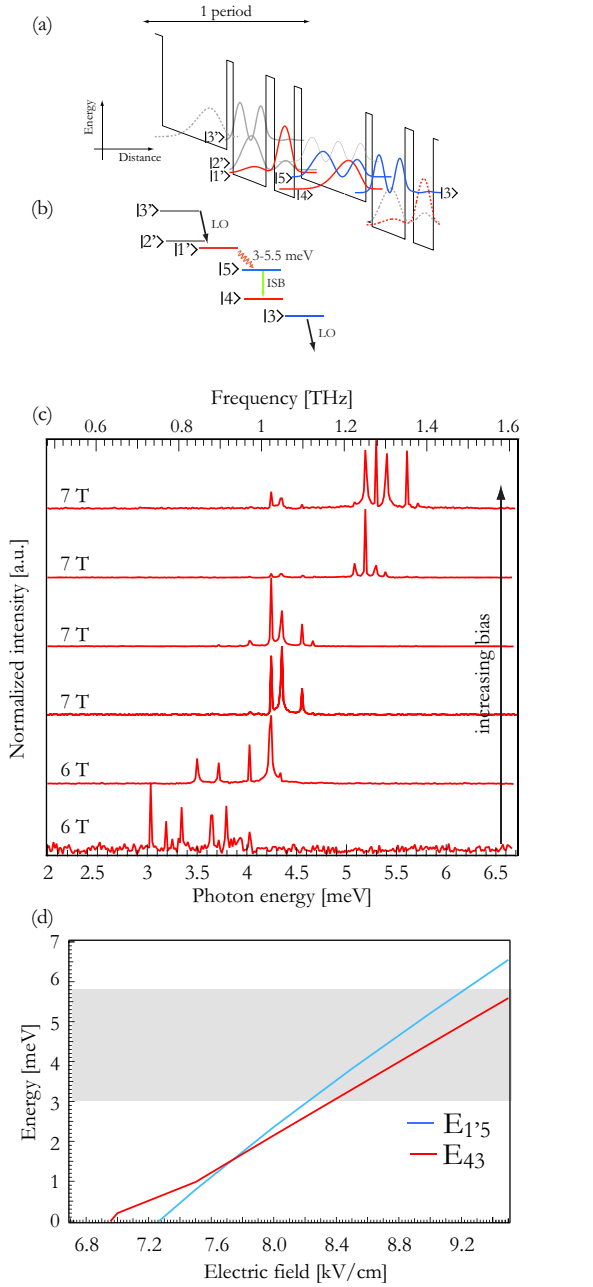

FIG. 2. (Color online) (a) Bandstructure calculation for the investigated structure for an applied electric field of 8.5 kV/cm, representative of the level arrangement after the NDR. (b) Schematic of the laser action: the injection mechanism is highlighted by a black arrow. (c) Laser emission spectra as a function of the applied magnetic field for increasing value of the bias. (d) Calculated values of the energy differences for the relevant low frequency transitions in the structure. The gray area represents the energies spanned by the low THz emission.

late that the majority of the electrons will be accumulated in the ground state $|1'\rangle$ after the NDR thus favoring the gain on the $|1'\rangle \rightarrow |5\rangle$ transition.

The computed dipole matrix element $z_{1'5}$ is small and bias dependent (2.2–1.3 nm), giving rise to very low values for the gain cross section $g_c = 7-2.5\times10^{-12}$ m (see note in Ref. 8). A long upper state lifetime can balance the losses of the broadband double metal resonator, evaluated at this frequency to be $\alpha_{tot} \simeq 5$ cm^{-1} with a two-dimensional FE modeling. It is important to note that in this case the carriers populate the upper state of the laser transition $|1'\rangle$ not by means of a resonant tunneling process but by being scattered from level $|3'\rangle$ mainly by LO phonons and from level $|2'\rangle$ by intersubband scattering.[9] Injection mechanisms based on scattering assisted transitions are reminiscent of the early proposals of an intersubband laser.[10] A phonon-assisted scheme has been realized for mid-IR devices[11] and recently in the THz by Kumar *et al.*[12] A photon-phonon scheme has been also realized on a two-well THz QCL,[13] and gain from injector states was predicted in Ref. 14. The magnetic field plays a crucial role in stabilizing electrically the structure. By inspecting the I-V curves reported in Fig. 1(c)–1(e) we note a change in the NDR shape as a function of the applied magnetic field. The emitted power at low frequencies (0.7–1.4 THz) can be estimated by comparing the signal detected in the same experimental setup at 0 T for the $|5\rangle \rightarrow |4\rangle$ transition. We can estimate a peak power of 3 mW for the low THz frequency emission. This indicates an high efficiency of

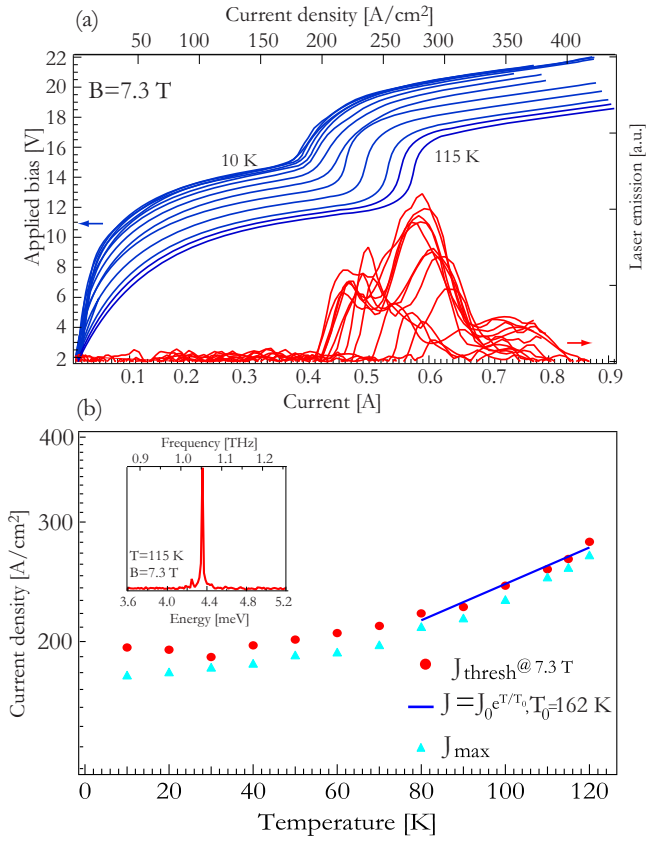

FIG. 3. (Color online) (a): L-I-V curves for an applied magnetic field of 7.3 T as a function of the heatsink temperature for a 1.6 mm long, 130 μm wide laser ridge. (b) Temperature dependence of the threshold current (dots) together with a fit with the function $J=J_0e^{T/T_0}$. The triangles represent the maximum current when resonantly injecting in the state $|5\rangle$ as a function of the temperature. Inset: spectral emission of the device at 115 K for an applied field of 7.3 T.

the laser (especially taking into account the 95% reflectivity of the facets at this frequency[15]) if compared with results obtained at similar frequencies in bound-to-continuum devices.[3]

The dependence of the low THz frequency laser emission on the temperature and the magnetic field has been also investigated. In Fig. 3(a) are reported the L-I-V curves in pulsed mode as a function of the temperature for an applied magnetic field of 7.3 T. The double-peaked shape of the L-I curve is most probably depending on the excited modes in the laser cavity. For another cavity width we do not observe such a shape [see Fig. 1(e)]. Laser action is observed up to a maximum temperature of 115 K, which corresponds to a high ratio $k_BT/h\nu \simeq 2.3$ between the thermal lattice energy and the photon energy. The experimental limit[16] constituted by the thermal energy for the operation of THz QCLs is overcomed by a combination of gain enhancement provided by the magnetic confinement and the peculiar injection scheme.

The threshold current as a function of the temperature is reported in Fig. 3(b); by fitting the points with the phenomenological relation $J(T)=J_0e^{T/T_0}$ we obtain a $T_0=162$ K, close to what observed in Ref. 5 where laser action at 1 THz was reported up to 215 K but for an applied magnetic field value of 30 T. In our case we believe that this weak temperature dependence of the threshold is mainly due to the injection mechanism rather than to the applied magnetic field value since the quenching of the phonon emission, which affects the upper state lifetime, is not as efficient for this relatively low magnetic field values.[2,18] Further insight into the laser operation is gained when plotting the temperature dependence of the maximum current density J_{max} when the structure is aligned to resonantly inject electrons in state $|5\rangle$ [in Fig. 3(b)]. The behavior of J_{max} is identical to the threshold current density of the diagonal transition. This indicates that the observed threshold behavior of the $|1'\rangle \rightarrow |5\rangle$ is mainly due to the non-resonant injection mechanism which leads to the charge cumulation in state $|1'\rangle$. The laser action stops because of thermal backfilling in state $|5\rangle$ since the intersubband scattering is not efficiently depleting the lower state at high ($T>115$ K, $\Delta E_{54}=13$ meV) temperatures. One attractive feature of a QC laser based on non-resonant injection and diagonal transition is the possibility to achieve lasing at very low frequencies since the injection mechanism is less sensitive to leakage currents which become more and more important as the subband energy spacing is reduced.[3,12]

In conclusion, laser action at 1 THz is observed up to 115 K for relatively low applied magnetic fields. A change in the injection scheme of the laser in combination with a strongly diagonal transition could represent an alternative direction in the design of THz QC lasers.

The author (G.S.) would like to thank S. Kumar and C. Walther for stimulating discussions. Financial support from SNF (Contract No. 200020-116749) is gratefully acknowledged.

[1] J. Faist, F. Capasso, D. Sivco, C. Sirtori, A. Hutchinson, and A. Cho, Science **264**, 553 (1994).
[2] A. Leuliet, A. Vasanelli, A. Wade, G. Fedorov, D. Smirnov, G. Bastard, and C. Sirtori, Phys. Rev. B **73**, 085311 (2006).
[3] G. Scalari, C. Walther, M. Fischer, R. Terazzi, H. Beere, D. Ritchie, and J. Faist, Laser Photonics Rev. **3**, 45 (2009).
[4] G. Scalari, C. Walther, L. Sirigu, M. Sadowski, H. Beere, D. Ritchie, N. Hoyler, M. Giovannini, and J. Faist, Phys. Rev. B **76**, 115305 (2007).
[5] A. Wade, G. Fedorov, D. Smirnov, S. Kumar, B. S. Williams, Q. Hu, and J. Reno, Nat. Photonics **3**, 41 (2009).
[6] G. Scalari, M. Amanti, M. Fischer, R. Terazzi, C. Walther, M. Beck, and J. Faist, Appl. Phys. Lett. **94**, 041114 (2009).
[7] G. Scalari, S. Blaser, L. Ajili, J. Faist, H. Beere, E. Linfield, D. Ritchie, and G. Davies, Appl. Phys. Lett. **83**, 3453 (2003).
[8] g_c is defined as in Ref. 17 For the calculation we assumed a linewidth $2\gamma_{1'5}=2$ meV.
[9] The same argument applies eventually to the $|4\rangle \rightarrow |3\rangle$ transition where electrons are injected by intersubband scattering from state $|5\rangle$.
[10] R. Kazarinov and R. Suris, Sov. Phys. Semicond. **5**, 707 (1971).
[11] M. Yamanishi, K. Fujita, T. Edamura, and H. Kan, Opt. Express **16**, 20748 (2008).
[12] S. Kumar, C. Chan, Q. Hu, and J. Reno, Paper CThU1, Proceedings of the Conference on Lasers and Electro-optics (CLEO-QELS), San Jose, 2010.
[13] G. Scalari, M. I. Amanti, C. Walther, R. Terazzi, M. Beck, and J. Faist, Opt. Express **18**, 8043 (2010).
[14] S. Lee and A. Wacker, Appl. Phys. Lett. **83**, 2506 (2003).
[15] S. Kohen, B. Williams, and Q. Hu, J. Appl. Phys. **97**, 053106 (2005).
[16] B. S. Williams, Nat. Photonics **1**, 517 (2007).
[17] J. Faist, F. Capasso, C. Sirtori, D. Sivco, and A. Cho, in *Intersubband Transitions in Quantum Wells: Physics and Device Applications II*, edited by H. Liu and F. Capasso (Academic, New York, 2000), Vol. 66, Chap. 1, pp. 1–83.
[18] N. Péré-Laperne, L. A. de Vaulchier, Y. Guldner, G. Bastard, G. Scalari, M. Giovannini, J. Faist, A. Vasanelli, S. Dhillon, and C. Sirtori, Appl. Phys. Lett. **91**, 062102 (2007).